Robust features of Atlantic multi-decadal variability and its climate impacts

Mingfang Ting,[1] Yochanan Kushnir,[1] Richard Seager,[1] and Cuihua Li[1]

[1] Atlantic Multi-decadal Variability (AMV), also known as the Atlantic Multi-decadal Oscillation (AMO), is characterized by a sharp rise and fall of the North Atlantic basin-wide sea surface temperatures (SST) on multi-decadal time scales. Widespread consequences of these rapid temperature swings were noted in many previous studies. Among these are the drying of Sahel in the 1960–70s and change in the frequency and intensity of Atlantic hurricanes on multi-decadal time scales. Given the short instrumental data records (about a century long) the central question is whether these climate fluctuations are robustly linked with the AMV and to what extent are these connections subject to changes in a changing climate. Here we address this issue by using the CMIP3 simulations for the 20th, 21st, and pre-industrial eras with 23 IPCC models. While models tend to produce AMV of shorter time scales and less periodic than suggested by the observations, the spatial structures of the SST anomaly patterns, and their association with worldwide precipitation, are surprisingly similar between models (with differing external forcing) and observations. Our results confirm the strong link between AMV and Sahel rainfall and suggest a clear physical mechanism for the linkage in terms of meridional shifts of the Atlantic ITCZ. The results also help clarify influences that may not be robust, such as the impacts over North America, India, and Australia. **Citation:** Ting, M., Y. Kushnir, R. Seager, and C. Li (2011), Robust features of Atlantic multi-decadal variability and its climate impacts, *Geophys. Res. Lett.*, *38*, L17705, doi:10.1029/2011GL048712.

1. Introduction

[2] Atlantic Multi-decadal Variability (AMV, also known as Atlantic Multi-decadal Oscillation, AMO) has attracted considerable attention in the climate research community in the past few years due to its wide-ranging climate impacts [e.g., *Enfield et al.*, 2001; *Sutton and Hodson*, 2005; *Knight et al.*, 2006; *Trenberth and Shea*, 2006; *Zhang and Delworth*, 2006; *Seager et al.*, 2010]. The complexity in understanding the impacts of the observed AMV stems, in part, from its concurrence with the century-long upward trend in North Atlantic SST, a trend that has been associated with global warming and attributed to anthropogenic forcing. Some researchers have questioned the existence of natural, multi-decadal, Atlantic-centered SST variability in observations [e.g., *Mann and Emanuel*, 2006]. They argue that the observed long-term SST fluctuations in the North Atlantic may be caused by a combination of greenhouse gas and industrial

and volcanic aerosol forcing. *Ottera et al.* [2010] suggested that the phasing of the AMV in the past 600 years appear to be largely governed by solar and volcanic forcings. *Knight* [2009], however, concluded that the AMV, as inferred from the forced climate response using the ensemble-mean of the CMIP3 models, is inconsistent with the observed AMV in 20th Century observations, thus supporting the existence of an unforced component of the AMV. One of the central questions is whether the unforced, multi-decadal Atlantic SST variability is separable from the radiatively forced SST variability during the 20th Century. *Ting et al.* [2009] used the CMIP3's multi-model/multi-ensemble 20th Century simulations to estimate the radiatively forced (both anthropogenic and natural) North Atlantic SST trend and confirmed the existence of natural multi-decadal SST variability over the North Atlantic in 20th Century observations. They have further shown that the spatial structures of the forced and internal North Atlantic SST variability patterns are distinct from each other and are each tied to unique world-wide precipitation anomalies. A recent study by *DelSole et al.* [2011] argues that there exists a global pattern of internal multidecadal variability, separable from the anthropogenic signal and centered in the Atlantic and that it contributes significantly to the global warming trend of the recent decades (1977–2008), thus further emphasizing the necessity to separate between and accurately account for the forced and internal SST patterns of variability in the North Atlantic.

[3] Given the short instrumental record of SST (~130 years) and the lack of reliable century long observations of global precipitation and atmospheric circulation, it is difficult to establish the robustness of the AMV's spatial and temporal structure and its impacts on precipitation. However, the availability of many climate model simulations from CMIP3, with prescribed 20th and 21st Century radiative forcing as well as with preindustrial conditions, offers a rich data set for understanding these issues within the model framework provided that the models also display the AMV. This study attempts to address particularly the following questions:

[4] 1. How robust is the spatial pattern of the AMV and its linkage to global precipitation as presented by *Ting et al.*'s [2009] observational analysis?

[5] 2. How well do climate models capture the natural Atlantic SST variability on multi-decadal time scales?

[6] 3. Does the nature of the models' AMV change with the changing radiative forcing?

[7] The paper is organized as follows. Following a brief description of data and methods in section 2, the detailed comparison of modeled and observed AMV and related precipitation and circulation patterns are shown in section 3, followed by the summary and conclusions in section 4. The results of signal to noise (S/N) maximizing EOF analysis of the CMIP3 models 20th and 21st Century simulations and

[1]Lamont-Doherty Earth Observatory, Earth Institute at Columbia University, Palisades, New York, USA.

the seasonal dependence of the AMV-associated surface temperature and precipitation patterns are presented in the auxiliary material.[1]

2. Data and Methods

[8]   In this study, we use the same signal to noise maximizing EOF analysis as by *Ting et al.* [2009] except that it is applied to an ensemble of all available CMIP3 model simulations for the 20th and 21st (A1b) Centuries. We used 23 CMIP3 models for both the 20th and 21st centuries and multiple realizations for some models, with a total of 75 multi-model ensemble members for the 20th and 54 for the 21st Century.

[9]   In addition to the 20th and 21st Century model simulations, 20 AR4 models, forced with pre-industrial greenhouse gas concentrations were used for the AMV analysis providing a comparison to the 20th and 21st Century simulations of AMV. These pre-industrial integrations are longer than one century and thus provide a robust estimate of the models internal variability, free of a time varying, external source of forcing. For the observed AMV patterns, we used the sea surface temperature data from the Goddard Institute for Space Studies (GISS) analysis of global surface temperature change [*Hansen et al.*, 2010], which uses the HadISST1 [*Rayner et al.*, 2003] from 1880–1981 and satellite measurements of SST from 1982 to the present (OISST.v2) [*Reynolds et al.*, 2002]. The global land precipitation and surface temperature were taken from the UEA CRU TS2p1 monthly datasets with $0.5° \times 0.5°$ resolutions [*Mitchell and Jones*, 2005].

[10]   The signal to noise maximizing EOF analysis [*Allen and Smith*, 1997] is applied to global SST for multi-model and multi-ensemble members of the CMIP3 simulations to determine the radiatively forced component of SST variability in the 20th and 21st centuries. Annual means of each model were filtered with a recursive low-pass filter with a cut off at 10 years prior to the EOF analysis. The time series associated with the leading, global S/N EOF (PC1) is taken as the time series of the radiatively forced component of SST. The spatial pattern of the forced components of SST is obtained by regressing the global SST onto the PC1 time series (see auxiliary material). The internal component of the North Atlantic SST (the AMV) index is then obtained as the residual of the observed North Atlantic basin-wide average SST after subtracting the forced component (see Figure S1 in the auxiliary material). The spatial patterns of surface temperature and precipitation associated with the internal North Atlantic SST on decadal to multi-decadal time scales are obtained by regressing these variables at each grid point onto the AMV index. The AMV index in the pre-industrial model runs are defined as the basin-wide average SST of the North Atlantic between the equator and 60N.

3. Results

[11]   To assess and compare the temporal properties of the internally varying, North Atlantic multi-decadal SST signal (the AMV) we calculated and compared the lagged autocorrelations of AMV index for each CMIP3 model for lags from zero to 35 years (Figures 1 (top left) and 1 (bottom

left), colored lines). The autocorrelation function (acf) of the observed AMV is shown as the solid black line in Figure 1 (top left). Note that the AMV indices in Figure 1 are only associated with natural climate variability internal to the coupled ocean-atmosphere system, as the component associated with the externally forced variability has been subtracted as described by *Ting et al.* [2009] as well as in the auxiliary material. The observed AMV (solid black line in Figure 1, top left) behaves similarly to a perfect sine function with a period of 70 years (black dot-dashed line in Figure 1, top left). The 5% significance intervals of the acf based on a century-long, low-pass filtered white-noise time series are shown in Figures 1 (top left) and 1 (bottom left) in dotted lines. While some of the models do not exhibit significant oscillatory behavior, about half of the CMIP3 models for the 20th Century and 16 out of 23 models of the 21st Century simulations do show autocorrelations above the noise level at varying lags, as is the case for the 20th Century observations. For models with significant autocorrelation above the filtered white noise level, the estimated periods of oscillation range from 20 to 80 years.

[12]   The similarity between the acf of observed AMV and that of the perfect sine function with a period of 70 years indicates the quasi-periodic nature of the observed AMV in the 20th Century with a period close to 70 years. This period estimate is consistent with that of *Schlesinger and Ramankutty* [1994] and *Delworth and Mann* [2000] who used a proxy reconstruction of surface temperature for the last 330 years. *Gray et al.* [2004] however, found AMV periods between ~40 and 128 years in their tree ring reconstruction from the 16th to the 20th Century with a peak at 42.7 years for the years 1856–1990. These varying estimates suggest that AMV does not have a single well-defined periodicity but varies across a range of decadal timescales. The CMIP3 model results support the above conclusion and further indicate the lack of oscillatory behavior in some of the models. The root-mean-square values of the AMV time series are shown (by model) in Figures 1 (top right) and 1 (bottom right). The amplitudes of the AMV in CMIP3 models are comparable to, or slightly weaker than, observed, with typical amplitudes ranging from $0.07°$ to $0.12°C$ as compared to about $0.15°C$ in 20th Century observations.

[13]   The spatial structures of the AMV in both models and observations are determined by linearly regressing the grid point surface temperature values onto the AMV index for each model and ensemble member and for the observations. The annual mean surface temperature regressions are shown in Figure 2a for observations, in Figure 2b for 20th, and in Figure 2c for 21st Century model simulations. We stippled the regions where 18 out of 23 (87%) models show an agreement in the signs of the regression coefficients to indicate the robustness of the results. The stippling in observations indicates the 95% confidence level using a Monte Carlo statistical significance test (as by *Ting et al.* [2009]).

[14]   The positive phase of the observed AMV is characterized by a comma-shaped surface temperature pattern in the North Atlantic with largest amplitude over the subpolar regions and an extension along the east side of the basin and into the subtropical North Atlantic (Figure 2a). The warming of the North Atlantic basin during the positive phase of AMV is significantly linked with warming over the southern U.S., the northwest coast of Africa and the Mediterranean. The CMIP3 models' 20th Century simulations reproduce the

---
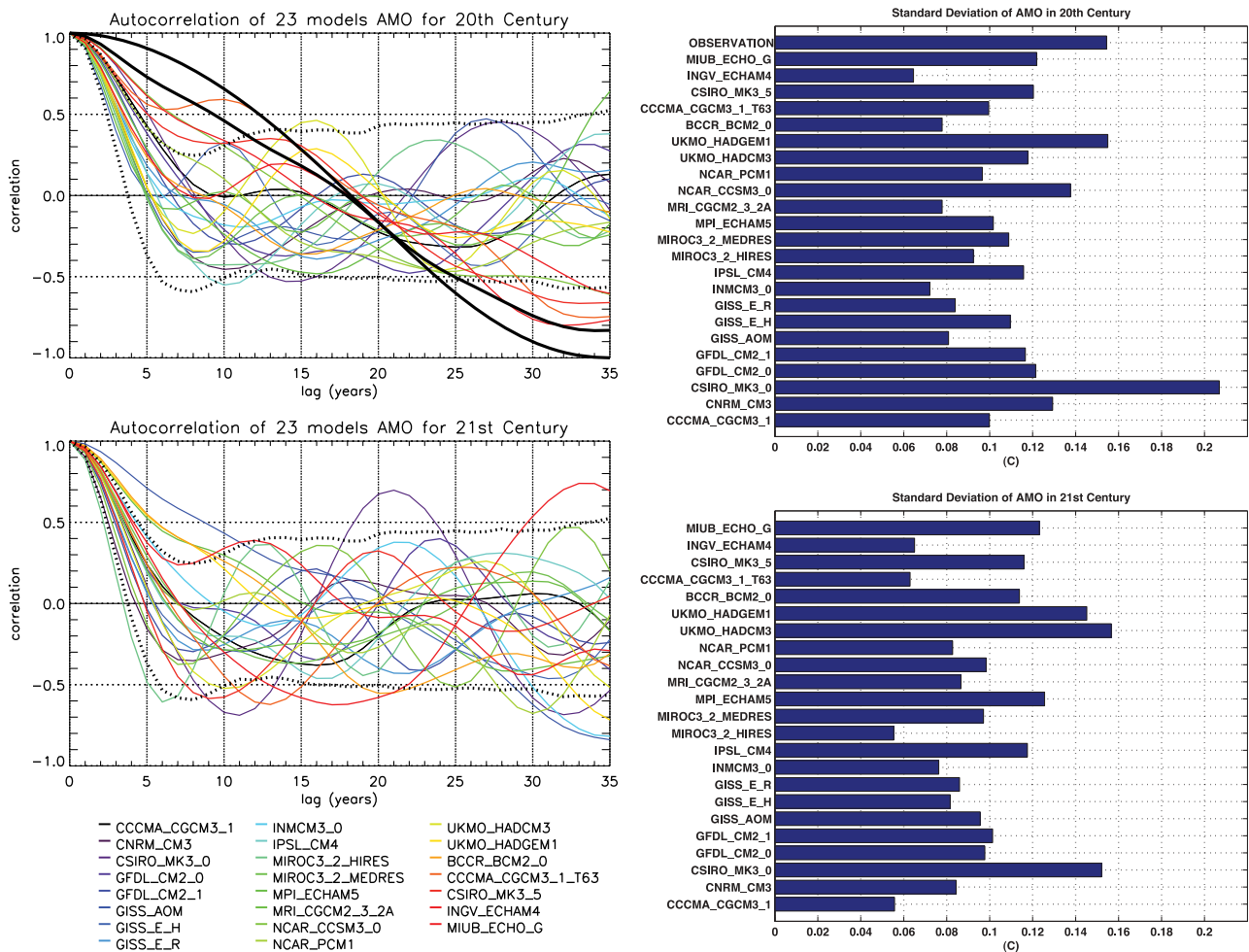
Figure 1. Autocorrelation of AMV indices in models (color lines) and observations (black line) with lags from zero to 35 years for (top left) 20th Century and (bottom left) 21st Century with A1b scenario. Black dot-dashed line is the auto-correlation when calculated for a perfect sine function with a period of 70 years, and the dotted black lines represent the 5% significance intervals at each lag based on autocorrelations of the filtered white noise time series. The keys for the color lines are indicated at the bottom on the left. (top right and bottom right) The corresponding amplitudes for the AMV indices.

AMV pattern very well (Figure 2b) with a similar shaped SST pattern in the North Atlantic. The amplitude of the tropical North Atlantic warming in the models is slightly weaker than in observations, while the subpolar amplitude is comparable. The models are highly consistent in showing a warming across the entire Northern Hemisphere. The discrepancies between 20th Century models and observations are mainly over the Eurasian continent and the tropical eastern Pacific where the models indicate a consistent warming while observations show a weak (and not significant) cooling. The AMV pattern remains consistent going from the 20th to the 21st Century A1b scenario simulations (compare Figures 2b and 2c), particularly over the North Atlantic and tropical eastern Pacific, indicating little change in AMV spatial structure as greenhouse gas forcing increases.

[15] To verify that the use of the S/N maximizing EOF procedure helps in identifying and successfully removing the radiatively forced signal in North Atlantic SST in the 20th and 21st Century model simulations and the 20th Century observations, we examined the AMV pattern and its association with precipitation using 20 CMIP3 pre-industrial model experiments. The AMV index is defined as the annual mean SST averaged over the North Atlantic from the equator to 60°N. The spatial pattern of the surface temperature regression averaged across the 20 models is shown in Figure 2d. The similarity between the pattern shown in Figure 2d and the patterns shown in the other panels of Figure 2 confirms that the analysis technique for removing the forced SST signal is valid.

[16] Figures 2e–2h show the spatial distribution of the regression coefficients of the precipitation at each grid point with the corresponding AMV index in the observations and various model configurations mentioned above. Similar to previous observational and modeling studies [e.g., *Enfield et al.*, 2001; *Sutton and Hodson*, 2005; *Knight et al.*, 2006; *Zhang and Delworth*, 2006; *Mohino et al.*, 2011], Figure 2e confirms that in observations the positive phase of AMV is associated with increased rainfall over the Caribbean, the Sahel, and the South Asian monsoon region and decreased rainfall over the southern United States, Mexico and tropical South America. There is also an indication of decreased rainfall over southern South Africa and Australia. In contrast to the observations, the models not only provide many more realizations (on the order of 50–70), but also offer global
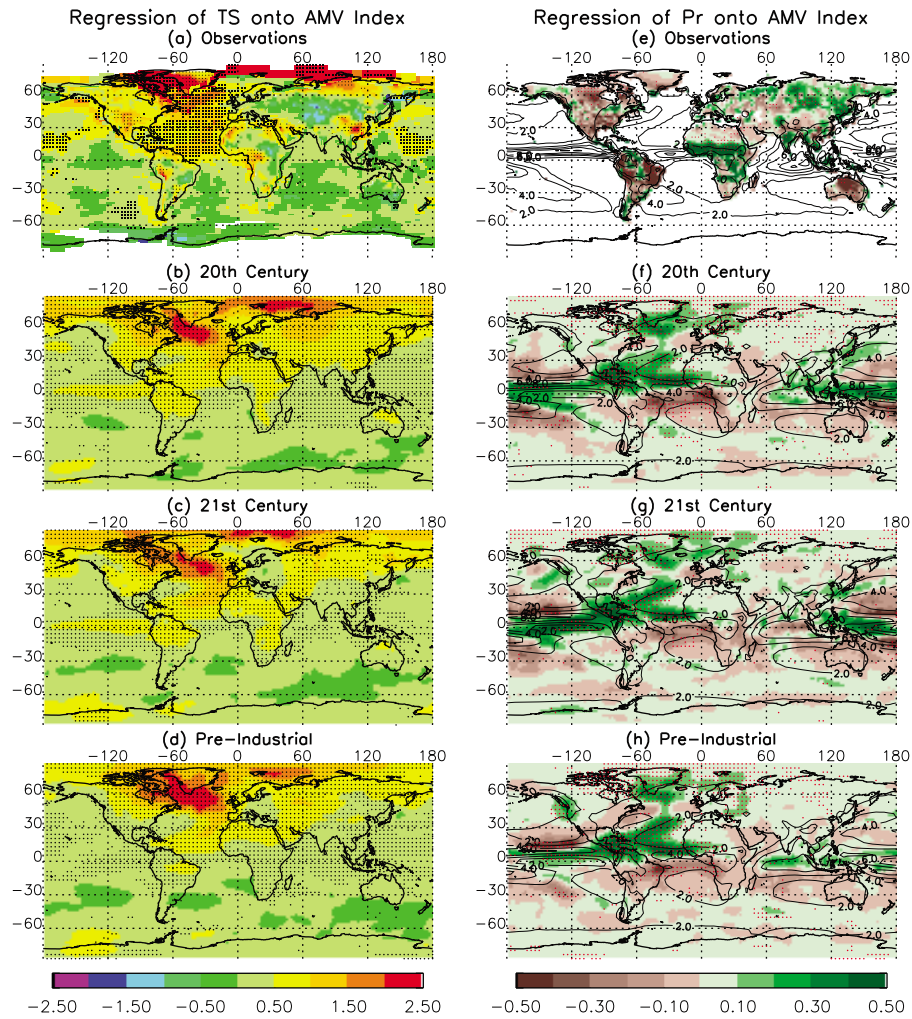
Figure 2. Global surface temperature regression onto the AMV indices for (a) observations, (b) 20th Century, (c) 21st Century with A1b scenario, and (d) Preindustrial CMIP3 model simulations. (e–h) Same as Figures 2a–2d, but for precipitation. Stippling in Figures 2a and 2e indicates 95% confidence level based on Monte Carlo test, in Figures 2b, 2c, 2f, and 2g indicates 18 out of 23 models showing the same sign regression coefficients, in Figures 2d and 2h indicates 16 out of 20 models showing the same sign regression coefficients. Contours in right panels are for climatological precipitation contoured at 2 mm/day intervals.

land and ocean coverage. The 20th Century model precipitation regressed onto the AMV time series and averaged over all 23 models is shown in Figure 2f. The Sahel rainfall anomaly, while weaker than in observations, is part of the change in tropical Atlantic rainfall and is consistent with a shift of the Atlantic ITCZ northward (in the warm phase), relative to its climatological position (indicated by solid contours). The Sahel rainfall anomalies associated with AMV is seen predominantly during Northern summer (JJAS) when the ITCZ is at its northernmost location (see auxiliary material). There is increased rainfall over the tropical Atlantic and the tropical eastern Pacific, consistent with the warm SST anomalies there. The drying over southwestern Africa and northeastern Brazil is also consistent with the northward shift of the Atlantic ITCZ and the increased north-south temperature gradient in the tropical Atlantic (Figure 2b). The models also consistently exhibit a dry tropical South America south of the equator [see *Seager et al.*, 2010]. The observed drying over North America during the AMV warm phase is limited and not consistent across models, unlike the response

in atmospheric general circulation models forced by prescribed warm tropical Atlantic SST anomalies [*Kushnir et al.*, 2010]. One possible explanation for this discrepancy is that, although the warm Atlantic would induce drying, the coupled 20th and 21st Century models display a warming of the equatorial Pacific, which would induce opposing wet conditions [*Seager et al.*, 2005]. In that respect we note that the pre-industrial runs display a weak AMV related Pacific warming and consistently exhibit more drying over North America (Figure 2h). In observations, warm Atlantic SSTs are associated with cool equatorial Pacific SSTs and a stronger drying over North America.

[17] Most of the precipitation features noted in the 20th Century model simulations are reproduced in the 21st Century simulations with similar magnitude (Figure 2g). Figure 2h shows the precipitation response to AMV as simulated in the pre-industrial era model simulations. The similarities between Figures 2f–2h indicate that the presence and the differing strength of the external radiative forcing did not alter the precipitation anomalies associated

with AMV. The wet sub-polar North Atlantic and south-ward shifted eastern tropical Pacific ITCZ corresponding to the positive phase of the AMV are robust across the CMIP3 model simulations under all three different external forcing scenarios, from the pre-industrial, 20th, and 21st Century conditions. The tropical Pacific precipitation anomalies associated with AMV in the models will themselves force precipitation anomalies around the globe meaning that the diagnosed precipitation-AMV relationship is a combination of both Atlantic and Pacific forcing of circulation anomalies. Lack of observed precipitation data over the oceans prevents a validation of this aspect of the models' AMV relationships but the associated modeled link to warm SSTs in the tropical Pacific is not supported by observations. There is a further disagreement between models and observations in that the barely significant observed wetting of India and drying of Australia associated with a positive AMV phase are not robustly reproduced in the CMIP3 model simulations.

4. Summary

[18] Using S/N maximizing EOF analysis, we successfully removed the forced component associated with both anthropogenic and natural (external) radiative forcing for the 20th and 21st Century CMIP3 model simulations resolving their naturally occurring multi-decadal North Atlantic basin-wide SST variability. The model consensus regarding the externally forced signal also helps in isolating the AMV pattern and time evolution in the observations. The models are able to produce decadal to multi-decadal scale variations over the North Atlantic with similar amplitude to that observed but with no robust periodicity as suggested in the 20th Century observations. The spatial structure of the AMV in the models, however, is very similar to the observations. It is characterized by a comma-shaped pattern in the North Atlantic with a sub-polar maximum extending southward along the east side of the basin to the tropical Atlantic. The CMIP3 preindustrial AMV is consistent in pattern and time scale with that of the 20th and 21st Century AMV, providing further support to the validity of our signal separation method and lends credence to the existence of a natural AMV phenomenon.

[19] The precipitation patterns associated with AMV are also robust across the pre-industrial, 20th and 21st Century model simulations, and favorably compare to the 20th Century observations. The predominant precipitation pattern associated with the positive phase of the AMV is a northward shifted Atlantic ITCZ, resulting in increased rainfall from the western Sahel across the tropical North Atlantic to Central America, and decreased rainfall from western South Africa across the tropical South Atlantic to eastern South America. Over the tropical eastern Pacific in the models, there is a robust southward shifted ITCZ associated with the warm phase of AMV which will itself further impact precipitation globally. However, this feature cannot be verified in observations although *Kushnir et al.* [2010] noted that on shorter timescales a warm tropical Atlantic is associated with a similar, yet weaker, shift of the ITCZ west of the shores of Central America in the recent satellite observed precipitation record. This is consistent with positive model SST anomalies in the tropical Pacific during positive AMV. However the observed positive AMV is associated with cold tropical Pacific SSTs. Consequently the realism of the AMV-tropical

Pacific link in models, and how it impacts global precipitation, is open to question.

[20] Previous observational studies have suggested that AMV has a marked impact on North American hydroclimate, causing anomalous drying across North America when AMV is in its positive phase [*Enfield et al.*, 2001; *McCabe et al.*, 2004]. The models have a less significant impact possibly because of the warm tropical Pacific SST anomalies that accompany a positive AMV. Similarly the 20th Century observations reveal more rainfall in the Indian monsoon region during positive AMV [*Goswami et al.*, 2006; *Zhang and Delworth*, 2006], but this is not consistent across the model simulations, again possibly because of the influence in the models of AMV on the tropical Pacific. The model simulations also indicate increased precipitation over Southern Greenland and the subpolar Atlantic as well as increased rainfall over the subtropical North Atlantic during the AMV warm phase.

[21] Our study adds important contributions toward the understanding of AMV: We show that there is a well-defined spatial pattern for AMV in the North Atlantic that is consistent in 20th Century observations as well as the climate model simulations of the 20th, 21st and pre-industrial conditions, albeit with differing temporal behavior of the phenomenon between model and observations. The AMV spatial and temporal structures are insensitive to the strength of the external radiative forcing from the pre-industrial condition to 21st Century scenario forcing. Furthermore, the models and observations agree on the important precipitation impacts of AMV over the tropical Atlantic basin, associated with a meridional shift of the Atlantic ITCZ. However the models do not support some of the observational features associated with a positive AMV, such as the drying over North America and Australia, and the wetting in the Indian monsoon region. This disagreement potentially follows from the differences in observed and modeled AMV-related features in tropical Pacific temperature (note that precipitation features cannot be evaluated due to absence of marine observations). More research is needed to untangle the links between the Pacific and Atlantic basins and how the two are coupled together via both atmosphere and ocean.

References

Allen, M. R., and L. A. Smith (1997), Optimal filtering in singular spectrum analysis, *Phys. Lett.*, *234*, 419–428, doi:10.1016/S0375-9601(97)00559-8.
DelSole, T., M. K. Tippett, and J. Shukla (2011), A significant component of unforced multidecadal variability in the recent acceleration of global warming, *J. Clim.*, *24*, 909–926, doi:10.1175/2010JCLI3659.1.
Delworth, T. L., and M. E. Mann (2000), Observed and simulated multidecadal variability in the Northern Hemisphere, *Clim. Dyn.*, *16*, 661–676.
Enfield, D. B., A. M. Mestas-Nunez, and P. J. Trimble (2001), The Atlantic multidecadal oscillation and its relation to rainfall and river flows in the continental U.S., *Geophys. Res. Lett.*, *28*, 2077–2080, doi:10.1029/2000GL012745.
Goswami, B. N., M. S. Madhusoodanan, C. P. Neema, and D. Sengupta (2006), A Physical mechanism for North Atlantic SST influence on the Indian summer monsoon, *Geophys. Res. Lett.*, *33*, L02706, doi:10.1029/2005GL024803.

Gray, S. T., L. J. Graumlich, J. L. Betancourt, and G. T. Pederson (2004), A tree-ring based reconstruction of the Atlantic Multidecadal Oscillation since 1567 AD, *Geophys. Res. Lett.*, *31*, L12205, doi:10.1029/2004GL019932.

Hansen, J., R. Ruedy, M. Sato, and K. Lo (2010), Global surface temperature change, *Rev. Geophys.*, *48*, RG4004, doi:10.1029/2010RG000345.

Knight, J. R. (2009), The Atlantic Multidecadal Oscillation inferred from the forced climate response in coupled general circulation models, *J. Clim.*, *22*, 1610–1625, doi:10.1175/2008JCLI2628.1.

Knight, J. R., C. K. Folland, and A. A. Scaife (2006), Climate impacts of the Atlantic Multidecadal Oscillation, *Geophys. Res. Lett.*, *33*, L17706, doi:10.1029/2006GL026242.

Kushnir, Y., R. Seager, M. Ting, N. Naik, and J. Nakamura (2010), Mechanisms of tropical Atlantic SST Influence on North American precipitation variability, *J. Clim.*, *23*, 5610–5628, doi:10.1175/2010JCLI3172.1.

Mann, M. E., and K. Emanuel (2006), Atlantic hurricane trends linked to climate change, *Eos Trans. AGU*, *87*(24), doi:10.1029/2006EO240001.

McCabe, G. J., M. A. Palecki, and J. L. Betancourt (2004), Pacific and Atlantic Ocean influences on multi-decadal drought frequency in the United States, *Proc. Natl. Acad. Sci. U. S. A.*, *101*, 4136–4141, doi:10.1073/pnas.0306738101.

Mitchell, T. D., and P. D. Jones (2005), An improved method of constructing a database of monthly climate observations and associated high-resolution grids, *Int. J. Climatol.*, *25*, 693–712, doi:10.1002/joc.1181.

Mohino, E., S. Janicot, and J. Bader (2011), Sahel rainfall and decadal to multidecadal sea surface temperature variability, *Clim. Dyn.*, doi:10.1007/s00382-010-0867-2.

Ottera, O. H., M. Bentsen, H. Drange, and L. Suo (2010), External forcing as a metronome for Atlantic multidecadal variability, *Nat. Geosci.*, *3*, 688–694, doi:10.1038/ngeo955.

Rayner, N. A., D. E. Parker, E. B. Horton, C. K. Folland, L. V. Alexander, D. P. Rowell, E. C. Kent, and A. Kaplan (2003), Global analyses of sea surface temperature, sea ice, and night marine air temperature since the late nineteenth century, *J. Geophys. Res.*, *108*(D14), 4407, doi:10.1029/2002JD002670.

Reynolds, R. W., N. A. Rayner, T. M. Smith, D. C. Stokes, and W. Wang (2002), An improved in situ and satellite SST analysis for climate, *J. Clim.*, *15*, 1609–1625, doi:10.1175/1520-0442(2002)015<1609:AIISAS>2.0.CO;2.

Schlesinger, M. E., and N. Ramankutty (1994), An oscillation in the global climate system of period 65–70 years, *Nature*, *367*(6465), 723–726, doi:10.1038/367723a0.

Seager, R., Y. Kushnir, C. Herweijer, N. Naik, and J. Velez (2005), Modeling of tropical forcing of persistent droughts and pluvials over western North America: 1856–2000, *J. Clim.*, *18*, 4065–4088, doi:10.1175/JCLI3522.1.

Seager, R., N. Naik, W. Baethgen, A. Robertson, Y. Kushnir, J. Nakamura, and S. Jurburg (2010), Tropical oceanic causes of interannual to multidecadal variability in southeast South America over the past century, *J. Clim.*, *23*, 5517–5539, doi:10.1175/2010JCLI3578.1.

Sutton, R. T., and D. L. R. Hodson (2005), Atlantic Ocean forcing of North American and European summer climate, *Science*, *309*, 115–118, doi:10.1126/science.1109496.

Ting, M., Y. Kushnir, R. Seager, and C. Li (2009), Forced and internal twentieth-century SST in the North Atlantic, *J. Clim.*, *22*, 1469–1481, doi:10.1175/2008JCLI2561.1.

Trenberth, K. E., and D. J. Shea (2006), Atlantic hurricanes and natural variability in 2005, *Geophys. Res. Lett.*, *33*, L12704, doi:10.1029/2006GL026894.

Zhang, R., and T. L. Delworth (2006), Impact of Atlantic multidecadal oscillations on India/Sahel rainfall and Atlantic hurricanes, *Geophys. Res. Lett.*, *33*, L17712, doi:10.1029/2006GL026267.

Y. Kushnir, C. Li, R. Seager, and M. Ting, Lamont-Doherty Earth Observatory, Earth Institute at Columbia University, 61 Rte. 9W, Palisades, NY 10964, USA. (ting@ldeo.columbia.edu)